Journal of *Marine Science and Engineering*

MDPI

Article

A Dynamic Trajectory Temporal Density Model for Analyzing Maritime Traffic Patterns

Dapeng Jiang [1,2], Guoyou Shi [1,2,*], Lin Ma [1,2], Weifeng Li [1,2], Xinjian Wang [1,3,*] and Guibing Zhu [4]

[1] Navigation College, Dalian Maritime University, Dalian 116000, China; dpj@dlmu.edu.cn (D.J.); malindmu@dlmu.edu.cn (L.M.); dmulwf@dlmu.edu.cn (W.L.)
[2] Key Laboratory of Navigation Safety Guarantee of Liaoning Province, Navigation College, Dalian Maritime University, Dalian 116026, China
[3] Liverpool Logistics, Offshore and Marine Research Institute, Liverpool John Moores University, Liverpool 999020, UK
[4] Maritime School, Zhejiang Ocean University, Zhoushan 316022, China; zhuguibing2020@zjou.edu.cn
* Correspondence: sgydmu@dlmu.edu.cn (G.S.); wangxinjian@dlmu.edu.cn (X.W.)

Abstract: This study investigates the spatiotemporal density aggregation and pattern distribution of vessel traffic amidst bustling maritime logistics scenarios. Firstly, a relatively new spatiotemporal segmentation and reconstruction method is proposed for ship AIS trajectories to address trajectory disruptions caused by berthing, anchorage, and other factors. Subsequently, a trajectory filtering algorithm utilizing time window panning is introduced to mitigate position jumps and deviation errors in trajectory points, ensuring that the dynamic trajectory adheres to the spatiotemporal correlations of ship motion. Secondly, to establish a geographical spatial mapping of dynamic trajectories, spatial gridding is applied to maritime traffic areas. By associating the geographical space of traffic activities with the temporal attributes of dynamic trajectories, a dynamic trajectory temporal density model is constructed. Finally, a case study is conducted to evaluate the effectiveness and applicability of the proposed method in identifying spatiotemporal patterns of maritime traffic and spatiotemporal density aggregation states. The results show that the proposed method can identify dynamic trajectory traffic patterns after the application of compression algorithms, providing a novel approach to studying the spatiotemporal aggregation of maritime traffic in the era of big data.

Keywords: temporal density; dynamic trajectory; geographical space; AIS; trajectory compression; traffic pattern

Academic Editor: Xinqiang Chen

Received: 26 January 2025
Revised: 16 February 2025
Accepted: 17 February 2025
Published: 19 February 2025

Citation: Jiang, D.; Shi, G.; Ma, L.; Li, W.; Wang, X.; Zhu, G. A Dynamic Trajectory Temporal Density Model for Analyzing Maritime Traffic Patterns. *J. Mar. Sci. Eng.* **2025**, *13*, 381. https://doi.org/10.3390/jmse13020381

1. Introduction

The rapid pace of socioeconomic development and the increasing frequency of international trade have established shipping as the dominant mode of transportation between ports worldwide. Within the waters of coastal countries or regions, vessels frequently entering and departing ports result in increased traffic volume. This phenomenon is particularly pronounced in sheltered navigation areas; waterborne traffic may even reach congested conditions. The study of maritime traffic situation awareness primarily focuses on vessel activities as the central research subject [1]. Traffic density is a quantitative indicator and can be employed to assess maritime traffic, reflecting issues within traffic patterns and facilitating further exploration of waterborne traffic data. Vessel density measurement should not rely solely on ship position counts but should incorporate multiple factors such as geospatial information, temporal cycles, and vessel activities. However, current

calculations may lack comprehensive consideration of these factors, leading to certain limitations in the research findings.

Vessel density is one of the main elements in the discipline of maritime traffic engineering, playing a pivotal role in the analysis of maritime traffic situations. Research on traffic density contributes to traffic planning management and route optimization. By analyzing the distribution of traffic flow density, maritime management departments can optimize route arrangement and the placement of maritime navigation aids, thereby reducing navigation risks and collision probabilities and minimizing interference and congestion among vessels [2]. The distribution of traffic density significantly impacts the assessment of maritime traffic safety. By identifying areas with high traffic density, high-risk zones in marine regions can be pinpointed, thereby enhancing the accuracy of maritime traffic risk assessments and reducing the occurrence rate of maritime traffic accidents [3]. Analyzing vessel density aggregation is advantageous for identifying potential risks and conflict points, providing data support for vessel collision avoidance and the avoidance of hazardous areas, thereby enhancing the level of maritime safety [4–6]. The research on maritime traffic density is also crucial in environmental impact assessment, as high-density traffic flows can result in increased traffic emissions, thereby affecting air quality [7]. Based on ship density distribution, it is possible to assess the extent traffic impacts marine environment and ecosystems, which can contribute to the development of effective marine conservation policies and management measures [8–10].

The analysis of vessel traffic density quantitatively reflects the level of congestion and hazard within marine areas. With the rapid development of digital maritime transportation, regional coverage Automatic Identification System (AIS) data and BeiDou Vessel Monitoring System (VMS) data have provided ample information for maritime traffic analysis. Additionally, amendments to the International Convention for the Safety of Life at Sea (SOLAS) have explicitly stipulated that vessels of different types must carry corresponding navigation equipment, including AIS devices capable of automatically providing information about the vessel to other vessels and coastal authorities [11]. Consequently, vessel AIS trajectory data have become the primary data source for maritime traffic engineering in the current big data era. In summary, the effective identification of maritime traffic flow and the distribution of its traffic structures based on AIS trajectory data is a crucial research topic in the current field of maritime traffic information analysis [12,13]. This study focuses on the impact of trajectory data with missing, noisy, and deviating points on the density analysis of marine traffic. The temporal characteristics of AIS trajectories are integrated into the study of the spatiotemporal density of marine traffic, addressing the limitations of the traditional density measurement process, which is based solely on counting the number of trajectory points within a limited region. This study provides a valuable research method for detecting the distribution of maritime traffic patterns and spatiotemporal density aggregation.

2. Related Work

2.1. Literature Review

AIS data exhibit distinct spatiotemporal characteristics, making the study of navigation patterns in critical waters through AIS data mining highly significant for maritime traffic management. Li et al. [14] investigate a spatiotemporal ship trajectory clustering method based on data mapping and density using AIS trajectories. This method demonstrates high accuracy in identifying typical navigation patterns and detecting abnormal behaviors. Rong et al. [15] introduce a data-mining-based approach for route characterization and anomaly detection, utilizing AIS data to establish a probabilistic model of vessel behavior. By identifying key navigation nodes, this method effectively extracts shipping patterns,

thereby enhancing maritime traffic management. Luo et al. [16] propose a ship trajectory classification method based on AIS data, enhancing classification accuracy by incorporating the Tsfresh module. The classified trajectories provide a foundation for traffic pattern distribution analysis. Additionally, the study emphasizes the importance of time-series features in trajectory analysis.

In the study of maritime traffic patterns based on AIS trajectories, spatiotemporal vessel density is an important research direction. It provides theoretical methods for fields such as vessel route planning and traffic risk area identification. Consequently, researchers have conducted studies on maritime traffic density or analyses of maritime traffic density related to vessel behavior. Willems et al. [17] were inspired by kernel density estimation techniques to obtain an overview density map of trajectory distributions through smoothing AIS trajectory, but the computational cost is high, and it requires a hardware solution to the problem. Meng et al. [18] utilized AIS data to analyze maritime traffic characteristics in the Singapore Strait. With line density expressed as unit area length and computed using specific equations, they explored the calculation of maritime traffic density through spatiotemporal density analysis. Natale et al. [19] characterized maritime traffic density by statistically analyzing the frequency of AIS message receptions. They utilized AIS data to create high-resolution density distribution maps of fishing vessel traffic, partitioning the water areas into grids and depicting fishing vessel density distributions across the entire water domain. Li et al. [20] employed compression algorithms to simplify the AIS trajectory for visualization efficiency. Building upon the simplified trajectory dataset, they utilized kernel density estimation methods to visualize vessel density.

Different studies have approached the investigation of maritime traffic density by considering various influencing factors. Liu et al. [21] developed a dynamic density calculation model, treating maritime traffic as a particle system. Drawing from the radial distribution function (RDF) in molecular dynamics, they computed the probability distribution of surrounding vessel atoms within a fixed distance from specified vessel atoms to characterize maritime traffic density. Yang et al. [22] expanded traditional maritime traffic density calculation by incorporating vessel length. They standardized the analysis by converting different ship lengths, noting their varying impacts on maritime density. The study assessed the capacity of specific water areas to accommodate vessels of different lengths. Lee et al. [23] utilized statistical density analysis based on AIS data to establish a framework for generating maritime traffic routes. They identified vessel waypoints based on density clustering and subsequently constructed routes by connecting these waypoints, serving as the basis for developing routes for autonomous surface vessels in marine environments. Lee and Yu [24] consider the impact of offshore wind farms on traffic and propose a novel method for determining route width based on offshore traffic distribution and line density analysis.

Current research on maritime traffic pattern analysis based on AIS trajectory data has made significant progress, covering multiple downstream directions such as density analysis, trajectory clustering, and anomaly detection. However, existing studies have not fully explored the spatiotemporal correlations in trajectory data, particularly the potential role of temporal features in the analysis of spatiotemporal density aggregation. This study places greater emphasis on modeling spatiotemporal correlations to enhance the accuracy and practicality of traffic pattern analysis.

2.2. Problem Analysis and Contributions

In summary, despite the abundance of literature on maritime traffic density or studies associated with it, there are still some issues with measuring maritime traffic density. Amidst the data explosion, trajectory data often contain noise, missing information, and

deviations from typical movement patterns. These factors compromise the accuracy, completeness, and continuity of vessel trajectory data, consequently exerting a negative impact on the study of maritime traffic density patterns.

In terms of model computation, current calculations of density on dynamic trajectories may suffer from inadequate precision. Some methods rely solely on the number of trajectory points and the area of the region to estimate density, thus ignoring the temporal attributes of vessel trajectories and the dynamic spatial distribution of trajectories. This also includes the failure to consider factors such as anchoring, berthing, or brief stops during vessel movement, resulting in an increased number of data points in trajectory records and consequently leading to inaccuracies in maritime traffic density calculations.

In the realm of spatial geographic data integration, few studies have incorporated spatial geographic information computation into the knowledge mining of maritime traffic patterns. There are distinct differences in traffic characteristics between open waters and port waters. Integrating spatial geographic data into traffic density measurement provides a novel modeling foundation for capturing local characteristics and density aggregation patterns of maritime traffic.

As we all know, trajectory data of vessel movements are closely linked with time. Analyzing density based on vessel trajectories during navigation can reflect the dynamic aggregation characteristics of maritime traffic. The main framework of this study is shown in Figure 1, and the contributions mainly include the following:

- A novel dynamic trajectory temporal density measurement model. By establishing a geographic spatial mapping of maritime traffic data and analyzing the temporal characteristics of trajectories, this study reveals dynamic vessel traffic aggregation patterns and quantifies spatiotemporal density.
- An effective method is devised for spatiotemporal segmentation and sub-trajectory reconstruction of vessel trajectory, addressing berth points, anchorage points, and various potential causes of spatiotemporal interruptions within moving trajectories to ensure the independence, integrity, and dynamism of trajectory sequences.
- A novel trajectory smoothing and filtering algorithm utilizing the time window panning method is introduced, primarily focusing on mitigating position jumping and deviation errors within time-continuous trajectory sequences.

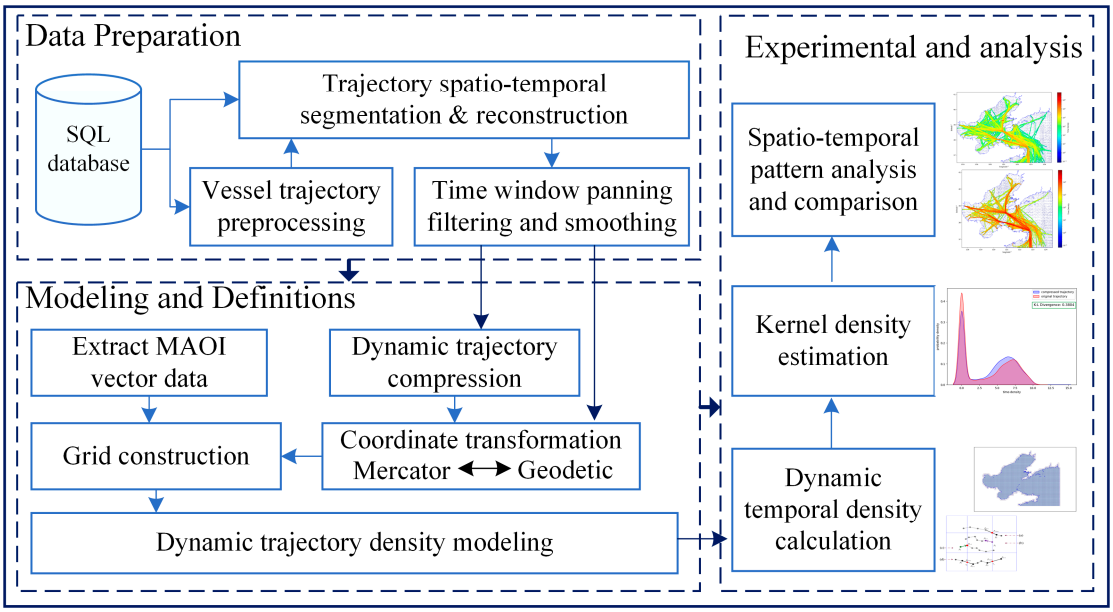

Figure 1. The framework of dynamic trajectory temporal density measurement method.

3. Methods

3.1. Data Preparation

Any data-based research has high requirements for the quality of data. AIS as a shipborne broadcast response system can provide a database for analyzing traffic activities in port and coastal waters. With the development of data storage technology, it has become possible to establish a regionalized and easy-to-access storage solution for the trajectory data of waterborne vessels. However, the AIS data stored in the database are raw data based on the receiver, and there are different types of problems in the temporal and spatial dimensions due to various reasons. In order to build a dynamic trajectory dataset, it is necessary to effectively process the moving trajectory data, including short-term mooring, anchoring, and spatiotemporal interruption caused by various factors. This section focuses on the removal of trajectory anomalies and noise points, the spatiotemporal segmentation and reconstruction of trajectories, as well as time window panning-based trajectory smoothing and filtering.

3.1.1. Vessel Trajectory Data Preprocessing

Due to various factors such as communication interference, inherent equipment problems, and human errors, AIS trajectory data suffer from issues related to physical integrity, spatial logical integrity, and temporal accuracy [25]. Transmission signal missing or drifting can result in localized data gaps within AIS trajectory sequences. Spatial logical integrity issues may arise from the following: (i) Due to random errors in longitude or latitude, the actual trajectory may spatially deviate from the logical positions expected from vessel motion characteristics, as depicted in Figure 2(1). (ii) The AIS devices installed on vessels are susceptible to vibrations from the ship itself or other external disturbances, leading to anomalous phenomena such as point jumps in trajectory data, as shown in Figure 2(2). (iii) The AIS trajectories of vessels should exhibit temporal continuity and positional sequence correlation under the same spatiotemporal conditions. However, data may be constrained by various factors, leading to the loss of consecutive data points within the same trajectory, resulting in unrelated trajectory sequences, as depicted in Figure 2(3).

To address the aberrations identified in the aforementioned trajectory data, this study implements a systematic preprocessing approach. Considering the irregular settings of AIS devices and the presence of fixed AIS devices at sea, which often have identification codes that do not comply with maritime mobile service identity (MMSI) coding standards (e.g., 0, 888888888, or 123456789), it is necessary to remove data entries with such erroneous identification codes from the dataset. Each trajectory sequence contains interrelated dynamic and static information. For trajectories affected by the scenarios described in (i), where the presence of random errors in any field would impact subsequent research, this approach involves directly removing these trajectories to ensure the completeness of trajectory dimensions. For trajectories that exhibit the anomalies described in (ii), this study introduces an effective time window smoothing and filtering algorithm in Section 3.2 below for rectification. If trajectory data exhibit scenario (iii), it is typically due to signal loss during transmission, resulting in separated trajectory segments associated with the same identification number. To ensure that each trajectory in the constructed trajectory dataset exhibits independence, continuity, and dynamism, this study proposes a novel method for spatiotemporal trajectory segmentation or sub-trajectory reconstruction to address these issues.

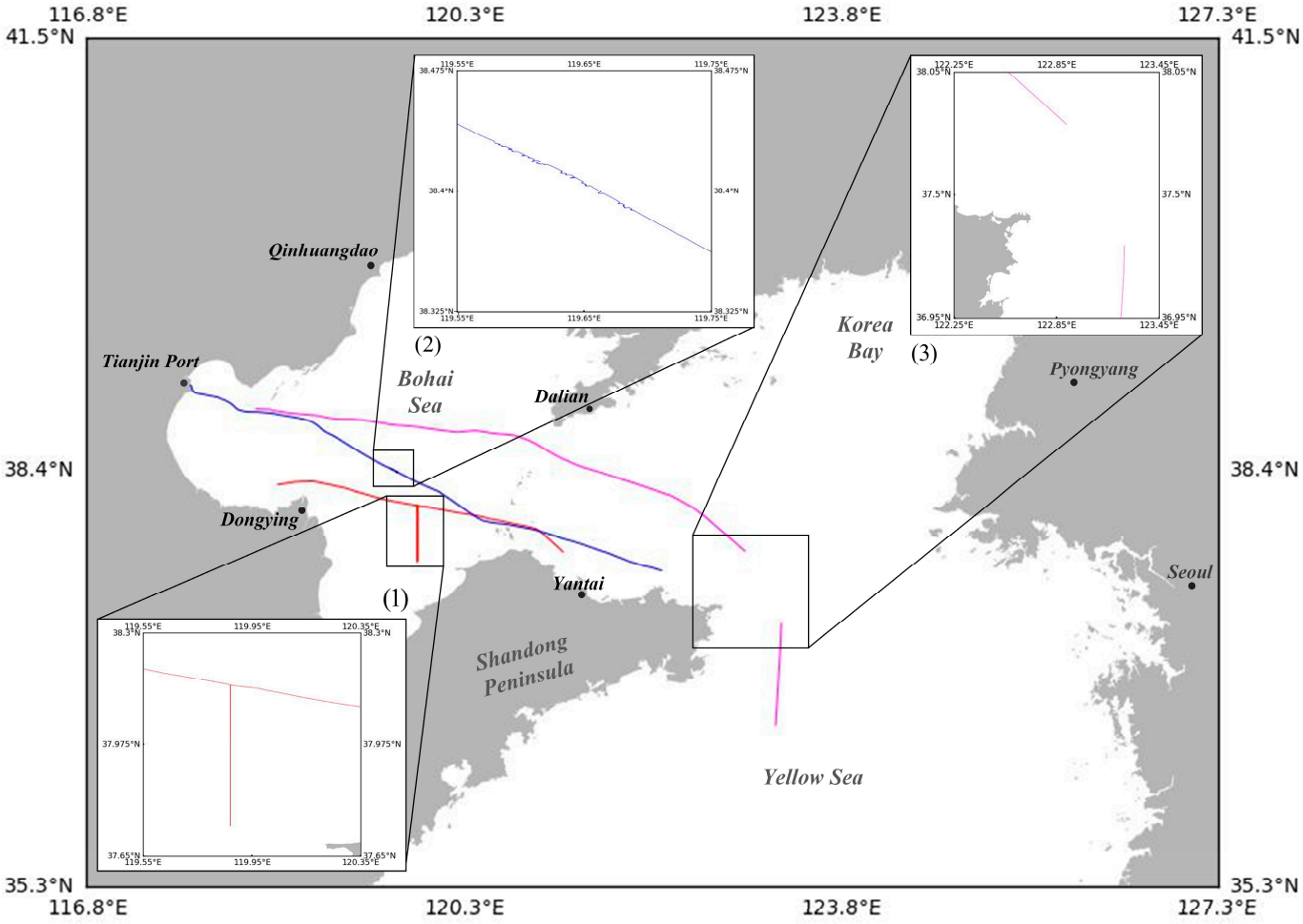

Figure 2. Several scenarios of vessel trajectory data with problems, Bohai Sea, China. (**1**) Trajectory points deviate from the logical positions. (**2**) Point jumps in trajectories. (**3**) Loss of consecutive trajectory points.

3.1.2. Trajectory Spatiotemporal Segmentation and Reconstruction of Sub-Trajectory

During the computation of dynamic vessel trajectory density, the temporal attribute plays a crucial role as a feature dimension. However, the decoded AIS data are stored in tabular form, with MMSI serving as the index. Consequently, when accessing specific trajectory entries, interrupted trajectories cannot be distinctly differentiated. Therefore, even after preprocessing, each trajectory still needs to be evaluated for spatiotemporal continuity. In addition to the local breaks outlined in Section 3.1.1 (iii), several other factors could cause interruptions in a sequence of vessel trajectories. Firstly, vessels with unique MMSI may repeatedly traverse fixed geographical boundaries over prolonged data collection or experimental periods, resulting in the segmentation of a continuous trajectory into multiple fragments. Secondly, the engineering vessel may undergo berthing at offshore platforms or brief periods of drifting, resulting in an increase in the number of position points in the localized area of the trajectory data corresponding to the MMSI. Measuring vessel density solely based on the number of AIS points using traditional statistical methods would yield inaccurate results. Therefore, it is necessary to conduct spatiotemporal discrimination and segmentation at the stop points in the trajectory intervals.

Since this study focuses on the research of dynamic traffic density aggregation patterns, it is important to construct a comprehensive dataset of vessel dynamic state trajectories. Therefore, addressing sequences of stop points within the trajectory is imperative. The reasons for the occurrence of stay track point sequences during a ship's journey at sea

include but are not limited to transshipment between land and sea facilities, short-term stops due to vessel malfunctions, accidents, and other factors. Unlike the phenomenon of stoppage of moving objects on land, different causes at sea produce different stay trajectories. Figure 3 illustrates two types of trajectory point sequences that may occur during a vessel's voyage at sea. In Figure 3a, the stop point p_i^k indicates a static period that may exceed a time threshold, often occurring during vessel emergencies. Another scenario, as depicted in Figure 3b, shows the stop sequence points $p_i^k \cdots p_j^k$, where the vessel stays due to a special event during navigation while the AIS equipment remains working, resulting in the generation of multiple trajectory sequence points within a small range. To address the potential occurrence of the aforementioned stop phenomena in trajectories, stop point detection algorithms can be applied for identification [26–28]. Applying this method effectively removes stop point sequences from trajectories, thereby ensuring the retention of trajectory sequences that depict the dynamic nature of vessel navigation. However, it may also introduce new trajectory interruption phenomena.

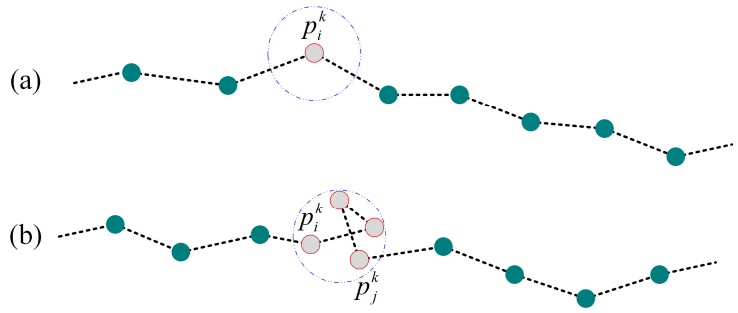

Figure 3. Schematic diagram of vessel trajectories for two possible stopping scenarios. (**a**) Static point. (**b**) Stop sequence points.

To address the trajectory interruption phenomena caused by the aforementioned reasons, this study proposes an effective algorithm for spatiotemporal trajectory segmentation and sub-trajectory reconstruction. By segmenting or reconstructing trajectories based on the spatiotemporal characteristics at the interruption points, this approach ensures that each data sequence maintains the continuity and independence of spatiotemporal trajectories during vessel motion.

A trajectory sequence dataset $D = \left\{P^k; (k = 1, 2, \ldots, N) \mid P \in \Theta\right\}$ is established based on the identification number MMSI, where Θ denotes the region of vessel trajectories, and P^k represents trajectory sequences of different MMSIs. For any trajectory segment, it can be represented as $P^k = \left\{p_1^k, p_2^k, \ldots, p_\tau^k, p_{\tau+1}^k, \ldots, p_T^k; \tau = 1, \ldots, T\right\}$, where P^k denotes the spatiotemporal information of trajectory points, and p_τ^k includes the spatiotemporal attributes $p = \{t_i, x_i, y_i, v_i, c_i; (i = 1, 2 \cdots, n)\}$, representing the longitude, latitude, speed, and course of the trajectory points at time t_i.

It is worth emphasizing that the decision to segment trajectories with the same MMSI primarily relies on the spatiotemporal correlation between points in the trajectory sequence. This study proposes logical operation discrimination rules defined by Equation (1) to segment or reconstruct trajectories, where 'seg' equals one, indicating the necessity for trajectory segmentation.

$$seg = \begin{cases} 1, \Leftarrow \begin{cases} (\delta t \geq T_{th2}) \cap (\delta d > 0) & \text{(1a)} \\ (T_{th1} \leq \delta t < T_{th2}) \cap (\delta d > D_{th}) & \text{(1b)} \end{cases} \\ 0, \Leftarrow \begin{cases} (T_{th1} \leq \delta t < T_{th2}) \cap (\delta d < D_{th}) & \text{(1c)} \\ (\delta t < T_{th1}) \cap (\delta d > 0) & \text{(1d)} \end{cases} \end{cases} \tag{1}$$

where δt represents the time difference between adjacent trajectory points, and δd represents the distance difference. The parameter T_{th} signifies the time threshold, while D_{th} represents the distance threshold. In this study, the threshold T_{th1} is determined according to the message transmission interval of 3 min when the vessel is anchored [29]. The threshold T_{th2} is determined based on the minimum time required for anchoring or mooring operations of a vessel. It is usually taken as the minimum empirical time required for the vessel to anchor or moor under the operation of the crew [30,31].

When the time span of the vessel trajectory dataset is long, the same vessel may re-enter the geographical area. In such instances, trajectory segmentation can be conducted using Equation (1a), and the resulting sub-trajectory segments should be considered as different voyages of the same vessel. If there is a period of signal loss in the trajectory sequence during which the vessel travels a significant spatial distance, the trajectory should be segmented according to Equation (1b) to ensure the continuity of the resulting trajectory sub-segments. For cases where there are stay points or stay sequences in the trajectory as shown in Figure 3, if the time difference and distance difference between adjacent trajectory points do not exceed the threshold, the logical discrimination described in Equation (1c) can be applied. In situation (a) of Figure 3, interpolation can be used to ensure the integrity of the trajectory. In situation (b) of Figure 3, after removing the stay point sequence, the average replacement point within the area can be calculated based on the points of the stay sequence. The attribute values of the average replacement points are derived from the average of the stay point sequence within the area. Otherwise, segmentation can be performed according to Equation (1a) or Equation (1b). The decision block diagram of the trajectory interval spatiotemporal correlation processing algorithm is shown in Figure 4.

3.2. Time Window Panning Filtering and Smoothing for Vessel Trajectory

Due to potential vessel vibrations or other signal interference during the transmission of AIS data, trajectory data may exhibit irregularities such as jagged, oscillatory, or juddering point distributions within a continuous time series, which do not conform to the expected trajectory characteristics of vessel motion. An example of this phenomenon is illustrated in the local trajectory segment indicated by the red arrows within the dashed box in Figure 5a, showing jagged, fluctuating, or jumping trajectory point distributions. To ensure that each trajectory or sub-trajectory accurately represents the true hydrodynamic motion state of the vessel, this study introduces a novel time window panning trajectory smoothing filter method. This method is designed to mitigate such issues by filtering and smoothing all trajectory datasets. A vessel trajectory is a time-series dataset that can capture changes in various characteristic states of the object based on its temporal dimension. Parameters such as position, speed, and heading are inherently dependent on temporal indexing. Consequently, following preprocessing steps including stay segmentation and trajectory reconstruction, the subsequent application of time window trajectory smoothing and filtering necessitates the establishment of a trajectory dataset based on vessel identification numbers. Here, $D = \left\{ P^k; (k = 1, 2, \cdots, N) \middle| P \in \Theta \right\}$ denotes the trajectory dataset, Θ represents the spatial domain of vessel trajectories, $P^k = \left\{ p_1^k p_2^k \cdots p_\tau^k p_{\tau+1}^k \cdots p_T^k; (\tau = 1, \cdots, \mathrm{T}) \right\}$ signifies the trajectory sequences associated with different MMSI, and $p = \{t_i, x_i, y_i, v_i, c_i; (i = 1, 2 \cdots, n)\}$ encapsulates the temporal attributes of longitude, latitude, speed, and course at a given time t_i.

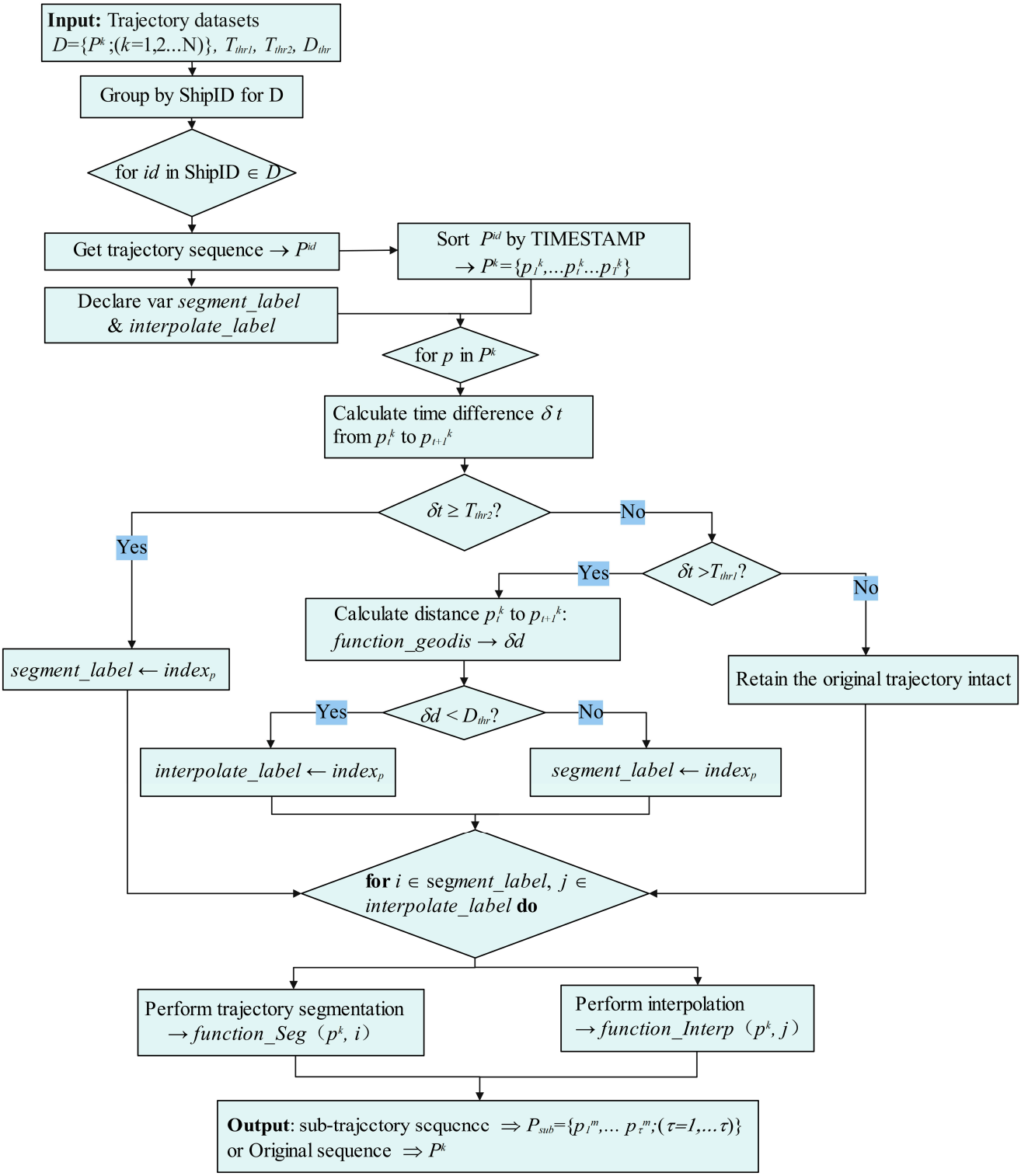

Figure 4. Decision block diagram of the trajectory interval spatiotemporal segmentation algorithm.

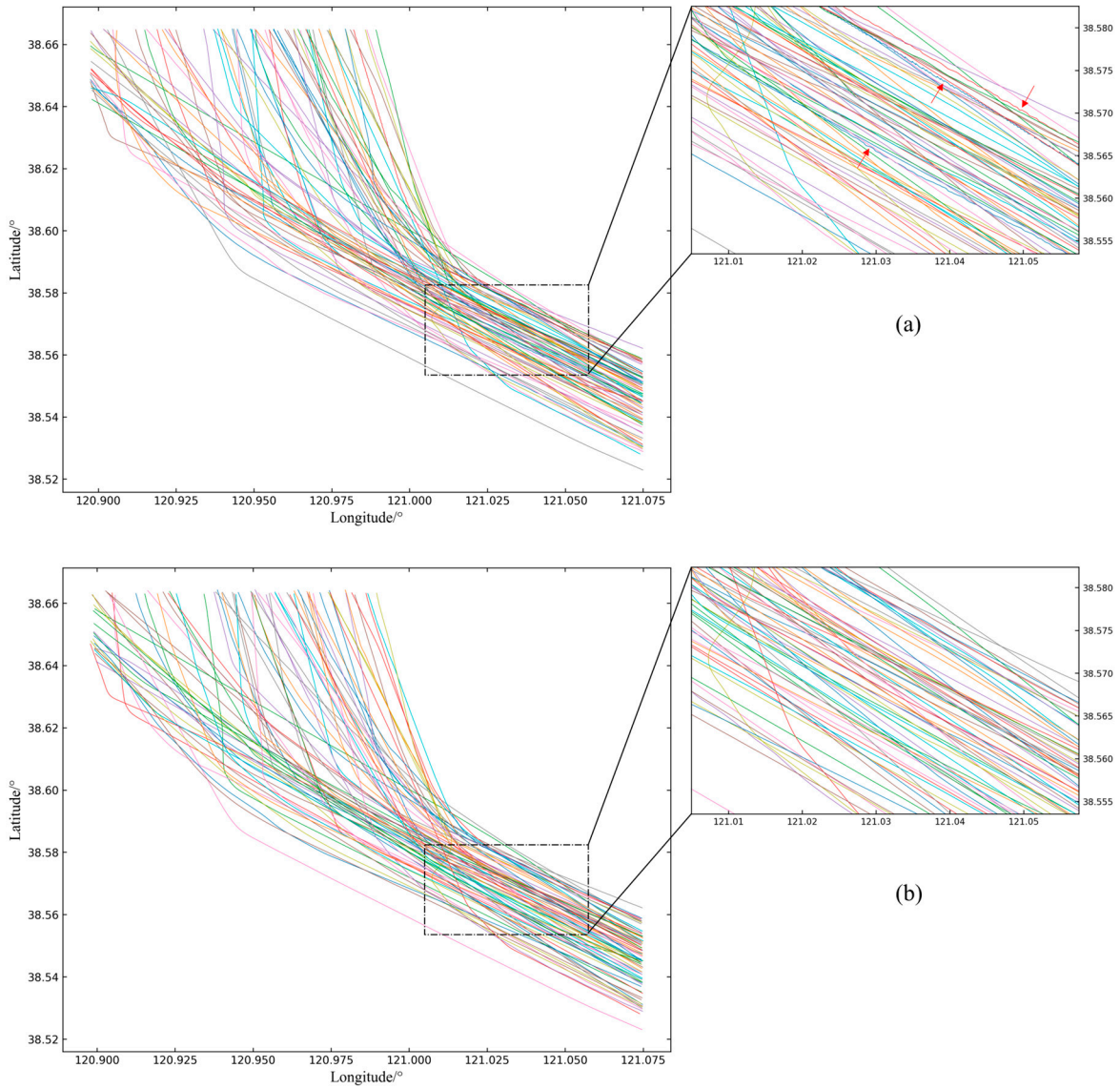

Figure 5. Comparison of time window panning trajectory smoothing effects. (**a**) Localization of anomalous trajectories with jagged and jumping points. (**b**) Corresponding localization after applying the time window panning trajectory smoothing algorithm.

The smoothing operation on trajectories requires algorithm design with a reference to the temporal dimension. When conducting trajectory smoothing, the first step involves establishing a time window. Within this time window, a time reference point is selected, sequentially corresponding to the order of time points in the window. A kernel function is then constructed by calculating the difference between the time within the window and the time reference point. This kernel function is applied to smooth the trajectory features corresponding to the traversed time. By panning the time window, the entire trajectory point feature data undergo filtering, gradually achieving the operation of smoothing and filtering for the entire trajectory segment. The moving step of the time window corresponds to the time interval between data points. When determining the size of the time window, considerations encompass the AIS transmission frequency and the sampling interval required by the model. In this study, the time window size is set to 60 s [32]. For the smoothing of continuous adjacent trajectory points, Gaussian kernel functions

are utilized to operate on the trajectory feature data within the window, as depicted in Equations (2) and (3).

$$\begin{cases} \delta T = t_{p_i} - t_r \\ \xi(t) = \frac{1}{\sqrt{2\pi}\cdot\Delta t_w} \cdot e^{-\frac{\delta T}{2\Delta t_w}} \end{cases} \tag{2}$$

$$\begin{cases} lon_s^i = \xi_i(t) \cdot P_{\Delta t}^k \left[lon_o^i\right] \\ lat_s^i = \xi_i(t) \cdot P_{\Delta t}^k \left[lat_o^i\right] \\ sog_s^i = \xi_i(t) \cdot P_{\Delta t}^k \left[sog_o^i\right] \end{cases} \tag{3}$$

where Δt_w represents the size of the time window, t_{p_i} denotes the time of the i point, while t_r represents the reference time within the window. $P_{\Delta t}^k$ represents the original trajectory sequence, while lon_o^i, lat_o^i, and sog_o^i represent the longitude, latitude, and speed of the trajectory point, respectively, within the time window. As illustrated in the local geographical area within the dashed box in Figure 5b, the trajectory data points exhibit a more uniform distribution after undergoing time window panning filtering and smoothing. In comparison to the original trajectory, the smoothed trajectory aligns more closely with the path of the object's motion, thereby effectively correcting deviations from the actual vessel trajectory.

3.3. Modeling and Definitions

3.3.1. Dynamic Trajectory Density Modeling

Most existing studies on maritime traffic density lack the dynamic and static data discrimination of trajectory sequences and ignore the temporal characteristics of trajectories. Consequently, it is unable to accurately characterize the spatiotemporal aggregation patterns of maritime traffic dynamics within geographic space.

The concept of vessel density serves as a metric to quantify the degree of ship concentration within marine areas. Definitions of ship density vary slightly across different literature sources. Generally, ship density refers to the count of vessels per unit area or length within a specified waterway or marine water. For instance, Wu and Zhu [33] defined ship density as the number of vessels present within a unit area of water at a given moment. Similar to studies conducted by [34], Dai et al. [35] have investigated ship density computation, primarily relying on the statistical analysis of AIS position points within geographical regions. Meanwhile, Liu et al. [21] proposed a ship density model based on radial functions inspired by molecular dynamics, which assesses the probability distribution surrounding stationary vessels. However, the model primarily focuses on micro-level analysis and does not consider the dynamic attributes of vessel trajectories.

This section proposes a maritime traffic flow density measurement method based on the travel time of vessel dynamic trajectories. By constructing a geographic grid within marine spatial regions, this method utilizes the travel time of vessels crossing geographical grid cells and considers the data transmission frequency under vessel navigation states. Subsequently, it computes the traffic density of vessel dynamic trajectories. Since the grid model is constructed based on geographic space, several scenarios may arise during the process of mapping trajectories onto the geographic grid, as illustrated in Figure 6. Each sub-grid within the geographic grid is assigned a unique identifier during construction. Vessel trajectories are denoted as $traj = \{p_1 p_2 \ldots p_k p_{k+1} \cdots p_n\}$, where each trajectory point is denoted as $p_i = (Id, t_i, lon_i, lat_i, c_i, s_i)$.

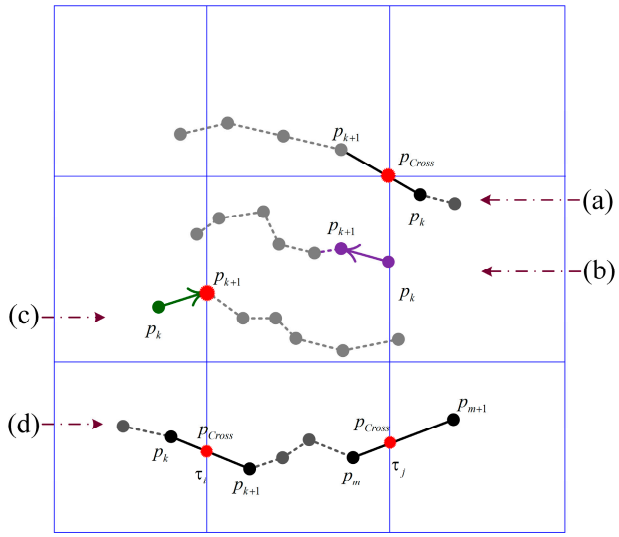

Figure 6. Schematic of the dynamic trajectory mapping geospatial grid.

If a trajectory contains a line segment $p_k p_{k+1}$ connecting adjacent points that pass through the vertex of a grid cell, the trajectory segment formed by the two consecutive points is split into two parts by the vertex. The sailing time of each part within the corresponding grid cell is calculated proportionally to the length of the trajectory segment and mapped to the respective sub-grid cells, as depicted in Figure 6a. If a position point p_k of a trajectory segment lies on the edge or vertex of a grid cell, the travel time of segment $p_k p_{k+1}$ is directly attributed to the grid cell mapped by p_{k+1}, as illustrated in Figure 6b. If a position point p_k of a trajectory segment lies within an independent grid cell, while the adjacent point p_{k+1} lies on the edge or vertex of a grid, the travel time of segment $p_k p_{k+1}$ is calculated based on the grid cell mapped by the previous point p_k, and a new traversal calculation starts from p_{k+1}, as shown in Figure 6c. In addition to the above scenarios, for any vessel trajectory, the travel time can be calculated based on the length of trajectory segments mapped by adjacent trajectory points in the geographic grid, as illustrated in Figure 6d.

3.3.2. Defining Marine Area of Interest

The identification of the marine area of interest (MAOI) is a key step in the dynamic trajectory temporal density study process. The MAOI in this study refers to the spatial intersection of the marine geographic waters, the area of busy maritime traffic that is manually delineated, and the land geographic extent, as depicted in Figure 7a. The geographic marine region vector data utilized in this study is sourced from the Flanders Marine Institute's website (https://www.marineregions.org/sources.php (accessed on 15 October 2024)), which provides the latest marine area data for exclusive economic zones (EEZs) worldwide [36]. However, the geographic layer of MAOI regions cannot be directly obtained from the website. Additionally, within the manually defined geographic boundaries, multiple adjacent exclusive economic zones of neighboring countries are involved, as shown in Figure 7b. The manually established geographic area encompasses parts of the North Sea of China, the northwest sea of North Korea, and the west sea of South Korea. Therefore, it is necessary to separately extract vector data for each marine region into individual files. Finally, the spatial geographic intersection operations are applied sequentially with the manually set polygonal geographic region to obtain the MAOI for research purposes, as illustrated in Figure 7c.

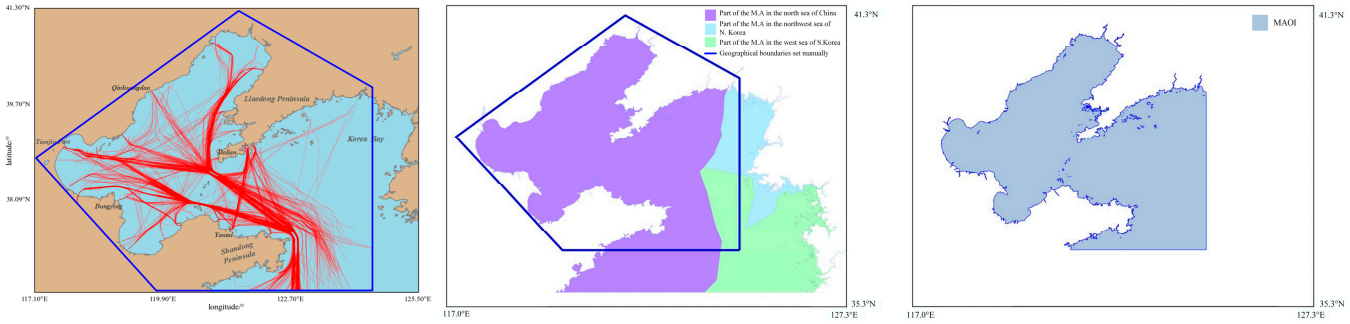

(**a**) (**b**) (**c**)

Figure 7. Maritime spatial distribution of busy traffic and MAOI vector data extraction. (**a**) Manually delineated geographic boundaries. (**b**) Spatial geographic layers of the EEZs of neighboring countries. (**c**) MAOI vector layer.

3.3.3. Coordinate Transformation

In this study, during the computation of the temporal density of dynamic trajectories mapped onto marine spatial geography, trajectory data, and geographical vector data are subject to interactive computation. Specifically, when vessel trajectories traverse geographical grids, it is often necessary to calculate intersection coordinates on a two-dimensional plane. To improve computational accuracy and facilitate the visual comparison of experimental results, the geographical coordinates of trajectory data and geographical vector data are converted into Mercator projection coordinates using Equation (4).

$$\begin{cases} x_N = k \ln\left[tg\left(\frac{\pi}{4} + \frac{B}{2}\right) * \left(\frac{1-e\sin B}{1+e\sin B}\right)^{\frac{e}{2}}\right] \\ y_E = k(L - L_0) \\ k = N_{B_0} * \cos(B_0) = \frac{a^2/b}{\sqrt{1+e'^2 * \cos^2(B_0)}} * \cos(B_0) \end{cases} \quad (4)$$

where (B, L) represents geographical latitude and longitude, respectively, while (x_N, y_E) represents the projected vertical and horizontal coordinates. L_0 denotes the origin longitude, B_0 denotes the standard latitude, N denotes the radius of curvature in the prime vertical, a denotes the semi-major axis of the ellipsoid, b denotes the semi-minor axis of the ellipsoid, e denotes the first eccentricity, and e' denotes the second eccentricity.

3.4. Dynamic Trajectory Compression

Typically, the analysis of maritime traffic flow density is conducted over a specific time period. During this period, the volume of vessel trajectory data increases exponentially due to the operational characteristics of AIS devices. This poses significant challenges to traditional methods, which rely on statistical analysis of vessel position points to assess maritime traffic density. If vessel trajectory data are compressed before density measurement, it becomes evident that traditional density measurement methods based on position points are not applicable, and accuracy cannot be guaranteed. However, in this study, even after trajectory data compression, traffic density measurement can still be achieved. This is because the calculation of vessel density in this study is based on the temporal attributes of dynamic trajectories. Therefore, the trajectory density calculation model constructed in this study enables the analysis and measurement of traffic density even with a reduced data volume.

3.4.1. DP Compression

The Douglas–Peucker algorithm [37] is a classical compression method, known for its ease of implementation, high efficiency in simplification, and favorable compression outcomes. Moreover, when the threshold is properly set, it achieves a high compression ratio. When

applying the DP algorithm to compress trajectories, selecting an appropriate threshold can effectively preserve both the overall and local features of the original trajectory without generating redundant points. As depicted in Figure 8, the compression principle of the DP algorithm is illustrated. Any vessel trajectory is represented as $traj = \{p_1 p_2 \dots p_k p_{k+1} \cdots p_n\}$. Initially, the anchor point (starting point) and floating point (ending point) of the trajectory are selected, forming a straight line segment $Ltr_{p_1 \to p_n}$ as the initial baseline, with a distance threshold set at $\varepsilon > 0$. Subsequently, the perpendicular distance between any point p_k in the interval trajectory sequence of anchor and floating points and its projection onto the line segment $Ltr_{p_1 \to p_n}$ is computed. The maximum distance value dp_k among these perpendicular distances is then selected. If $dp_k > \varepsilon$, the trajectory point corresponding to the maximum perpendicular distance is retained, thereby dividing the original trajectory into two sub-trajectory segments, $Ltr_{p_1 \to p_k}$ and $Ltr_{p_k \to p_n}$, with the floating point of $Ltr_{p_1 \to p_k}$ and the anchor point of $Ltr_{p_k \to p_n}$ being designated accordingly. Conversely, if $dp_k < \varepsilon$, all points between the anchor and floating points are discarded, retaining only the first and last points. This process is iteratively repeated on each sub-trajectory segment until the distance of all points from the baseline is less than ε, at which point the compression process halts.

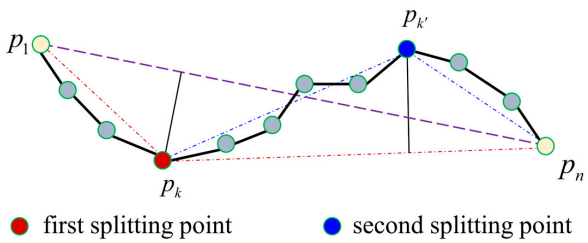

Figure 8. The schematic of DP algorithm trajectory compression.

After the data processing described in Section 3.1, each trajectory datum in the dataset is identified by MMSI and represents a complete and independent voyage trajectory sequence. The application of the DP algorithm to compress the dataset aims to reduce the size of the trajectory dataset while preserving its characteristics [38]. Moreover, it enables the measurement of maritime traffic density using compressed trajectory data [39]. When applying compression algorithms to trajectories, the influence of threshold values on compression effectiveness is a key consideration. A larger threshold results in fewer remaining trajectory points after compression, thus retaining less valuable information [40]. To preserve key feature points of trajectory sequences while balancing the effectiveness of trajectory compression with the accuracy of dynamic trajectory density measurement, this study analyzes changes in compression ratio during compression and computes the average compression error, as depicted in Figure 9.

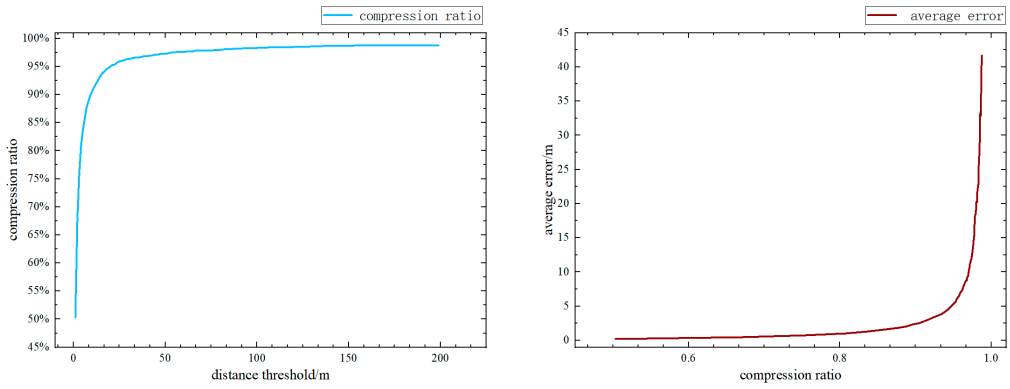

(**a**) Compression rate curve (**b**) Compression error curve

Figure 9. Indicator curves of trajectory compression.

3.4.2. Related Indicators Definitions

(a) Compression ratio. The trajectory compression ratio (TCR) indicates the rate of discarded trajectory points after compression to the total number of trajectory points before compression. The compression ratio for a single trajectory can be denoted as TCR; TCR is calculated according to Equation (5).

$$TCR = (n_{Tr} - m_{Tr'}) \cdot 100\% / n_{Tr} \tag{5}$$

where n_{Tr} denotes the number of trajectory points in the original trajectory, while n_{Tr} represents the number of trajectory points after compression.

(b) Average compression error. The average compression error (ACE) serves as a metric for assessing compression effectiveness. It refers to the cumulative sum of distances from the discarded points to their respective baselines upon each threshold update during the compression process, ultimately divided by the total number of trajectory points. $p_i = \{t_i, x_i, y_i; (i = 1, 2 \cdots, n)\}$ represents points in the original trajectory Tr, $p_j = \{t_j, x_j, y_j (j = 1, 2 \cdots, m)\}$ denotes points in the compressed trajectory Tr', $q_k = \{t_k, x_k, y_k; (k = 1, 2 \cdots, n - m)\}$ signifies the sequence of points discarded during compression, and ACE is calculated according to Equation (6).

$$ACE = \frac{1}{n} \sum_{g=1}^{m-1} \sum_{k=1}^{n-m} f_{dis}(q_k, l_g^{Tr'}), 1 < g \leq m - 1 \tag{6}$$

where the function $f(a, L)$ represents the perpendicular Euclidean distance from point a to line L, and $l_g^{Tr'}$ denotes the line segment between adjacent points in the compressed trajectory.

Additionally, unless otherwise specified, in this study, the term compression ratio refers to TCR, while average compression error refers to ACE.

3.4.3. Determination of Compression Threshold

Based on the definitions of compression ratio and average compression error metrics, this study applies the DP algorithm to a complete and independent dynamic trajectory within the MAOI and conducts an analysis of compression ratio and compression error. As shown in Figure 9a, an increase in the distance threshold leads to a gradual rise in the compression ratio but plateaus when the compression rate reaches 0.95. Simultaneously, with the increase in compression ratio, the average compression error also increases. When the compression ratio reaches 0.95, the average compression error sharply increases, as illustrated in Figure 9b. It is evident that further increasing the compression distance threshold would lead to the loss of essential trajectory features.

Dynamic trajectories may reflect significant spatiotemporal characteristics due to the geographical constraints on traffic flow distribution, such as large-angle steering and crossing routing systems. This section analyzes the compression effects on three selected trajectories. These trajectories cover the journey from the open sea to inland waters and then to the vicinity of ports, as well as the voyage from ports to the open sea. The DP compression was applied to each trajectory using a distance threshold corresponding to a 95% compression rate. Figure 10a displays scatter plots of three trajectories before and after compression, depicted using Mercator projection coordinates. In the plots, blue dots represent original dynamic trajectory points, while red hollow dots denote retained points after compression. As depicted in Figure 10b, the compressed trajectories preserve the primary characteristic points of the original trajectories.

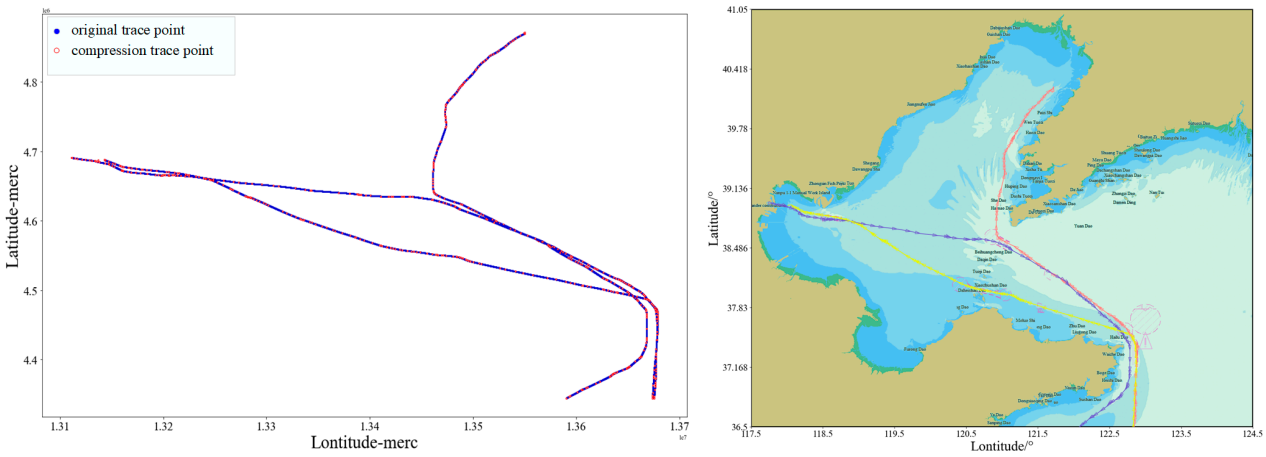

(**a**) Mercator scatter display (**b**) Geographic display of electronic chart

Figure 10. Example of the effectiveness of three dynamic trajectories after compression.

To determine the appropriate threshold, the preservation of key feature points in the compressed dynamic trajectories is examined. Here, the compressed trajectories are plotted on electronic navigational charts based on the WGS84 coordinate system, incorporating information such as positions and headings, as depicted in Figure 10b. From Figure 10b, it is evident that critical trajectory feature points, including turning areas, caution areas, and traffic lanes, are preserved within the vessel trajectories entering and leaving the inland sea. Therefore, considering the objectives of this study and taking into account the comparative results of threshold determination in the literature [41,42], along with the analysis and experimentation of compression indicators in this section, the compression thresholds in the dynamic trajectory compression process in this study are determined based on distance thresholds corresponding to a compression ratio of 95%.

3.5. Similarity Analysis Based on Kernel Density Estimation

To validate the feasibility of the proposed model, this section applies kernel density estimation (KDE) to analyze the computation results of traffic temporal density in the dynamic trajectory density model. KDE is a non-parametric statistical method used to estimate probability density functions. This method is applicable when it is not possible to assume a specific distribution for the given set of samples. The objective of KDE is to derive a probability density estimate at each data point by employing a kernel density function centered around it. The strengths of KDE include its robust handling of uncertainty pertaining to data distribution, its elimination of the necessity to presuppose a particular form of data distribution, and its applicability to multidimensional datasets. For a given dataset, the formula for KDE can be expressed as the weighted sum of kernel functions at each data point. Specifically, for a sample set $\{x_1, x_2, \ldots, x_n\}$ consisting of n observed values, the KDE function $\hat{f}(x)$ can be represented as Equation (7):

$$\hat{f}(x) = \frac{1}{n \cdot h} \sum_{i=1}^{n} K\left(\frac{x - x_i}{h}\right) \tag{7}$$

where h represent bandwidth parameter, n is the number of samples, and $K(\cdot)$ represents kernel function

In practical applications, Kullback–Leibler (KL) divergence is commonly used for model comparison and probability distribution fitting. It serves as a measure to gauge the disparity between the two models if there exist two discrete probability distributions P and Q. When utilizing the probability distribution Q to approximate the probability distribution P, there is an inevitable loss of information due to the disparity between the

two distributions, and KL divergence quantifies this loss of information. The zero value indicates identical distributions with no information loss. Conversely, larger KL divergence values indicate greater differences between the two distributions, reflecting increased information loss. Smaller KL divergence values imply minor discrepancies between the distributions, resulting in less information loss and a greater degree of similarity between them. The KL divergence between the two kernel density estimates is defined in accordance with Equation (8):

$$D_{KL}(P_o \parallel Q_c) = \sum_x p_o(x) \log\left(\frac{p_o(x)}{q_c(x)}\right) \quad (8)$$

where $p_o(x)$ and $q_c(x)$ represent two probability density functions, while x represents the density value of the random variable.

4. Case Study and Experimental Comparison

4.1. Dynamic Trajectory Temporal Density Calculation and Spatiotemporal Pattern Analysis

Traditional methods for calculating traffic density rely on counting the number of trajectory points within a region in a discrete manner, utilizing only the spatial attributes of the trajectories. Consequently, data generated by behaviors such as anchoring, berthing, and short stops are treated as noise or redundant data, which imposes limitations on the study of dynamic traffic density patterns using these conventional methods.

In Sections 3.1 and 3.2, this study effectively addresses the noise and redundant data in the trajectories, resulting in a dataset of complete and independent trajectory sequences. The model is based on the temporal attributes of the trajectories, computing the cumulative travel time of vessels in the navigational state within geographic grid cells. Therefore, this study explores the dynamic spatiotemporal density of maritime traffic. This dynamic temporal density intuitively reveals the distribution of potential spatiotemporal traffic patterns within the geographic space, including main routes and various branches. When quantifying vessel density, the expected number of vessels in a geographic area over a given period can be calculated by considering the AIS data sampling frequency.

4.1.1. Grid Construction in Geographic Space

It is necessary to construct a grid for the geographical space. The size of the geographical grid is determined by considering factors such as the distribution range of the geographical space, the broadcast frequency of AIS, and the average time and distance between adjacent trajectory points. Geographical grids within marine spatial regions are uniformly constructed with the boundaries of the MAOI serving as the delineating limits. Since maritime traffic flow is confined to marine waters, it is crucial to exclude geographical grids outside the marine domain. By constructing grids within the boundary range of the geographical space, it performs an intersection operation between the grid data and the MAOI vector layer data generated earlier in the text. This operation yields the grid data layer within the MAOI geographical region, as illustrated in Figure 11a. In order to fully cover the vessel traffic data in the geographic marine space, when processing the intersection of the MAOI geographic data layer and the grid data layer, the entire cell at the edges in the grid vector data intersecting with the MAOI is preserved, as illustrated in Figure 11b.

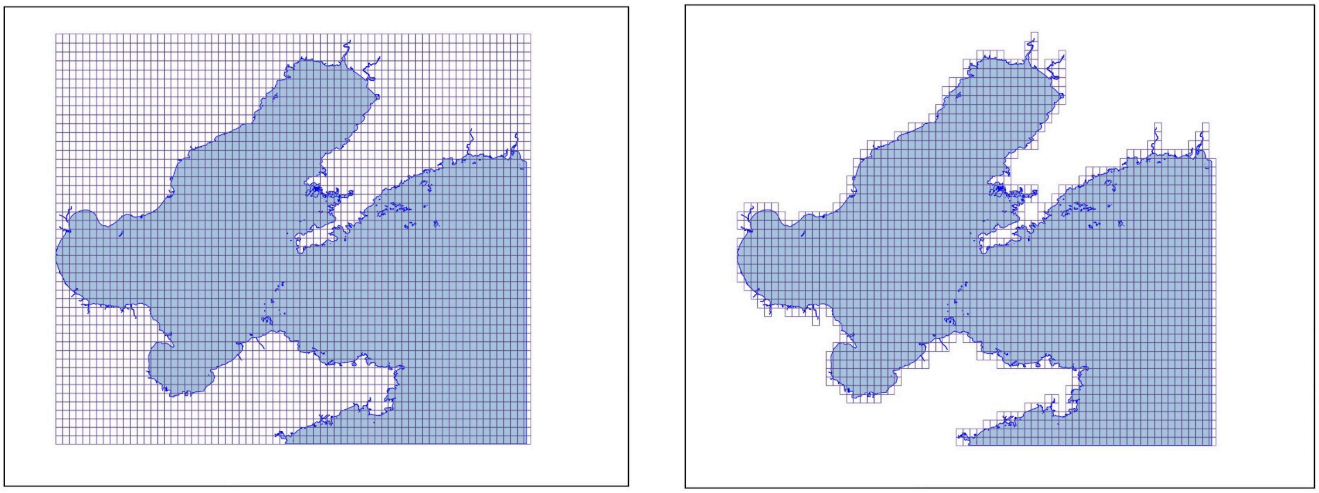

(**a**) The geospatial grid vector layer (**b**) The MAOI layer with geographic grids

Figure 11. Schematic diagram for constructing a geospatial grid vector layer based on MAOI regions.

Furthermore, when constructing the geographical space grid, this study divides the geographical space using the WGS84 geographic coordinate system as a reference to ensure navigational universality. The constructed geographical space grid vector data are stored in the form of point coordinate data for each grid unit. Since the calculation of dynamic density requires solving for the intersection points between trajectory segments and grid cell edges, both the trajectory data of maritime vessel traffic and the geographical grid vector point data constructed in this section are transformed into Mercator coordinate data format according to Equation (4) to enhance the accuracy of the computation.

4.1.2. Dynamic Temporal Density Calculation of Spatiotemporal Trajectory

Within trajectory sequences, each trajectory point contains multiple attributes such as position, time, speed, and course. By calculating the distance and duration between consecutive trajectory points, one can determine the distance covered and the duration of travel for each vessel within geographical grid units during a certain period. In addition, the method constructed in this study to measure the distribution of ship traffic density based on the spatial and temporal characteristics of the trajectories can also be utilized to recalculate the density after trajectory compression. This approach enables the exploration of traffic flow density distribution patterns while reducing the volume of data.

When a trajectory is compressed, resulting in a reduction in the sequence of trajectory points and an increase in the number of micro-trajectory segments with larger time intervals between adjacent points, a situation arises where the continuous line connecting trajectory points passes through two or more geographical grid units when mapped onto the geographical space. In such cases, it becomes necessary to perform intersection operations on the projection plane. The line connecting two trajectory points intersects successively with the edges of the geographical grid units it traverses. By calculating these intersections on the projection plane, the intersection points, along with the trajectory points at both ends, can be used to determine the sailing distance and time of each trajectory segment within the associated geographical space grid.

For each spatial grid cell in geographical space, spatial distance values are derived from the lengths of trajectory segments within each grid cell traversed by trajectories, thus allowing for the computation of temporal values. Similarly, cumulative distance values of vessel traffic flow crossing geographical area grids within a given time period can be computed for each subdivided sub-grid. This enables the determination of the dynamic

trajectory temporal density values of the geographical region. A notable feature of this study is that it no longer measures traffic density by counting the number of trajectory points. Instead, travel time is quantified based on the actual navigational distances covered by consecutive trajectory points. Additionally, the method established in this study, which measures the density distribution of vessel traffic based on the spatiotemporal characteristics of trajectories, also enables the recalculation of density after trajectory compression. This approach facilitates the exploration of traffic density distribution patterns while reducing data volume.

As depicted in Figure 12, utilizing vessel trajectories in the navigational state within a one-week timeframe as the dataset, this study applies the model to measure the density of maritime traffic flow in the Bohai and Yellow Seas of China. Figure 12a illustrates the effectiveness of applying the density model to compute the density of dynamic trajectories in the navigational state, while Figure 12b depicts the effect of applying the same model to trajectories compressed using the DP algorithm. From Figure 12a, it is evident that the application of the temporal density model effectively captures the distribution of maritime traffic density patterns and clearly delineates spatial variations in density within the geographical space. Additionally, it is worth noting that applying the density analysis model proposed in this study to measure compressed vessel trajectories in a dynamic navigational state can similarly reflect the distribution patterns and density discrepancies of maritime traffic. Moreover, it can provide a clearer depiction of the spatial orientations of main routes, feeder routes within the region, and the concentration of traffic route densities, as shown in Figure 12b.

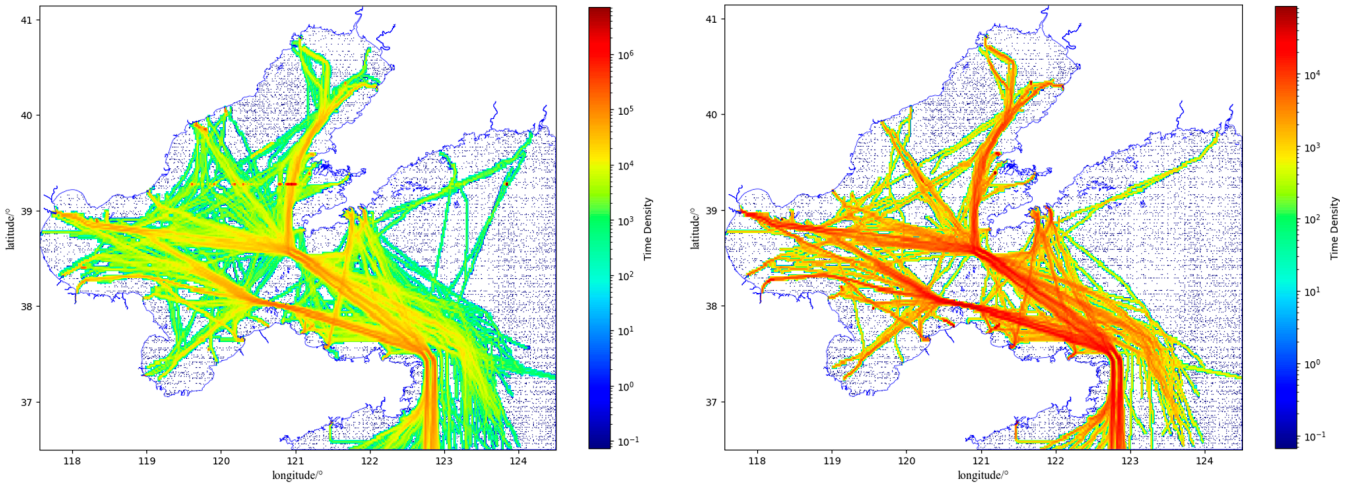

(**a**) Uncompressed dataset (**b**) Compressed dataset

Figure 12. Distribution of temporal density patterns of dynamic trajectories of ships at sea during a one-week period.

4.2. Effectiveness Analysis of Trajectory Temporal Density

After applying DP compression to vessel trajectories, this study utilizes the density model to analyze the temporal density distributions of traffic flow within marine waters. To evaluate the impact of the compression algorithm on the effectiveness of the dynamic trajectory temporal density model in measuring maritime traffic density, this section employs kernel density estimation to analyze the temporal density of traffic trajectories before and after compression, following the methodology described in Section 3.5. Furthermore, this section employs KL divergence to analyze the similarity of KDE curves, thereby further validating the robustness and effectiveness of the temporal density model in measuring traffic flow density in this study.

KL divergence is a method used to measure the difference between two probability distributions, calculating the relative entropy from one distribution to another. In this section, the temporal density probability distribution of uncompressed dynamic navigational trajectory data are defined as P, and that of the compressed dynamic navigational trajectory data are defined as Q. The similarity between the two temporal density distributions is then analyzed using the KL divergence, as presented in Equation (8).

Figure 13 illustrates the probability kernel density estimation of vessel dynamic trajectories within the MAOI region over a one-week period, corresponding to Figure 12. The spatial grid scale is set to 0.02°. To mitigate the impact of extremum on the overall data, reduce skewness in the distribution, and decrease the variance of the data for statistical analysis, a logarithmic transformation is applied to the density values calculated by the model within the geographic space. The blue and red colors represent the probability density estimation plots of compressed and uncompressed dynamic trajectory data, respectively. It can be observed from Figure 13 that the probability kernel density plots, derived from the density calculation model proposed in this study, exhibit similar shapes, distributions, and peak positions for both types of trajectory data measurements. The steep peak around zero signifies an abundance of zero and low-density values within the overall distribution of density values, while the remaining data, excluding zeros, demonstrate a trend toward a normal distribution. This suggests the existence of additional regions with high-density data. The calculation of the KL divergence value for the kernel density probability distributions of the two distinctively processed datasets yields merely 0.38. This indicates a substantial resemblance between the probability distributions of temporal density before and after trajectory compression. Such findings underscore the efficacy of employing the trajectory dynamic temporal density model proposed herein for analyzing traffic pattern distributions in compressed trajectories.

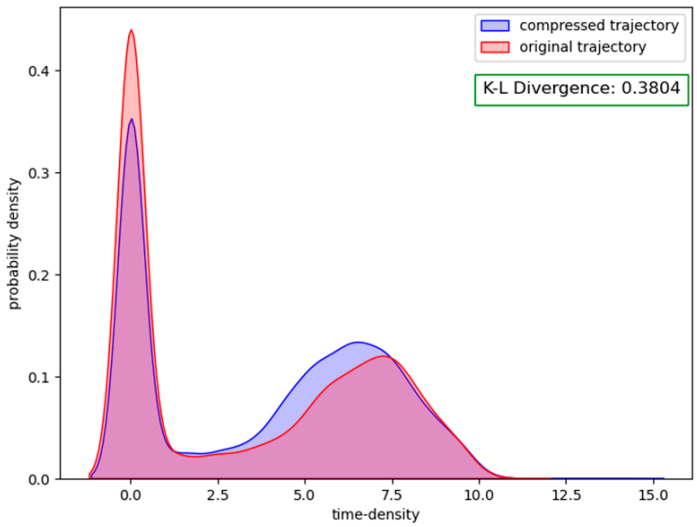

Figure 13. Probabilistic kernel density estimation plot.

4.3. Comparison of Trajectory Temporal Density at Different Spatial Scales

The spatial distribution characteristics exhibit significant heterogeneity across different regions. Employing grids of varying scales can better reflect this spatial heterogeneity. Selecting appropriate grid sizes is crucial to ensure the accuracy and reliability of the analysis results. Geographic grids of different scales can offer varying spatial resolutions, whereas larger-scale grids can provide a more macroscopic view of spatial information, suitable for analyzing global trends in traffic density aggregation. On the other hand, smaller-scale grids can offer more detailed spatial information, facilitating the exploration of local fea-

tures. Naturally, larger-scale grid data entail lower computational loads, thereby enhancing data processing and computational efficiency. Conversely, smaller-scale grids significantly increase computational complexity but offer more detailed and refined spatial information. Hence, striking a balance between data processing and computational efficiency is essential when determining grid scale sizes.

By comparing the analytical results at different scales, a more comprehensive understanding of the characteristics of traffic flow density distribution can be attained. Figure 14 illustrates the dynamic trajectory temporal density distribution computed using grids of varying sizes. In this section, focusing on the spatial distribution of environmental positions within the MAOI area, geographic spatial scales of 0.05°, 0.02°, and 0.01° are employed to investigate the traffic flow characteristics within the region. Figure 14a,c,e depict the temporal density traffic distribution maps of uncompressed dynamic vessel trajectories, while Figure 14b,d,f represent the temporal density traffic distribution maps after compression. As seen from the comparison of the subfigure in Figure 14, measuring maritime traffic flow at a larger spatial resolution can only capture the coverage of trajectories and the predominant traffic patterns, as illustrated in Figure 14a,b. At a smaller spatial resolution, not only can it reflect the distribution of traffic patterns, but it can also depict the actual traffic flow branches within the MAOI. The deeper the shade of red, the higher the frequency of vessel traffic passing through the geographic grid, indicating a longer duration of occupancy in that geographical area. This also signifies a higher traffic density in the corresponding geographical space, as illustrated in Figure 14c,d. When measuring the dynamic density of maritime traffic in a given area at a spatial resolution of 0.01°, it becomes evident that the spatial distribution patterns of vessel traffic within the region are clearly reproduced, with distinct contrasts in temporal density distribution. Particularly noteworthy is the clear depiction of bidirectional tributary density aggregation within the same main stream of vessel traffic. Additionally, high-density traffic patterns near ports are accurately represented, as illustrated in Figure 14e,f.

Additionally, it is evident that the temporal density measurement, based on the original dynamic trajectory as the data source, effectively illustrates the differential distribution of maritime traffic modes across different spatial locations. This observation is made during the process of setting up spatial resolution analyses at the three scales. Figure 15a–c depicts the probability kernel density distribution curves of temporal density measurements for traffic flow at spatial scales of 0.05°, 0.02°, and 0.01°, respectively. The blue curves represent the probability distribution curves of temporal density after compressed trajectories at the same spatial scale, while the red curves represent the probability distribution curves of temporal density for uncompressed dynamic trajectories. Correspondingly, the KL divergence values are quite small, measuring 0.35, 0.38, and 0.07, respectively, indicating a strong similarity between the two datasets. This also demonstrates that the dynamic trajectory temporal density model proposed in this study can analyze the aggregation patterns of maritime traffic states based on both original and compressed trajectories.

The dynamic trajectory density model proposed in this study aimed at mapping the dynamic voyage time of vessels' trajectories within the geographic space. Experimental comparisons show that when applying the method of this study to analyze the traffic patterns in the inland sea waters, setting the spatial scale of 0.05° only can find the main routes, which cannot detect the local branching patterns. By adjusting the spatial scale of 0.02°, a clear detection of branching traffic patterns and a balance of computational efficiency can be achieved. When the scale is set to 0.01°, it would increase the cost of computation considerably, and a small spatial scale is generally not chosen except for the application of detecting a limited region. In addition, while applying the compressed trajectories from the same source data, the method proposed in this study is still able to

detect the traffic temporal density pattern distribution, which provides an effective method for the trouble caused by a large amount of data.

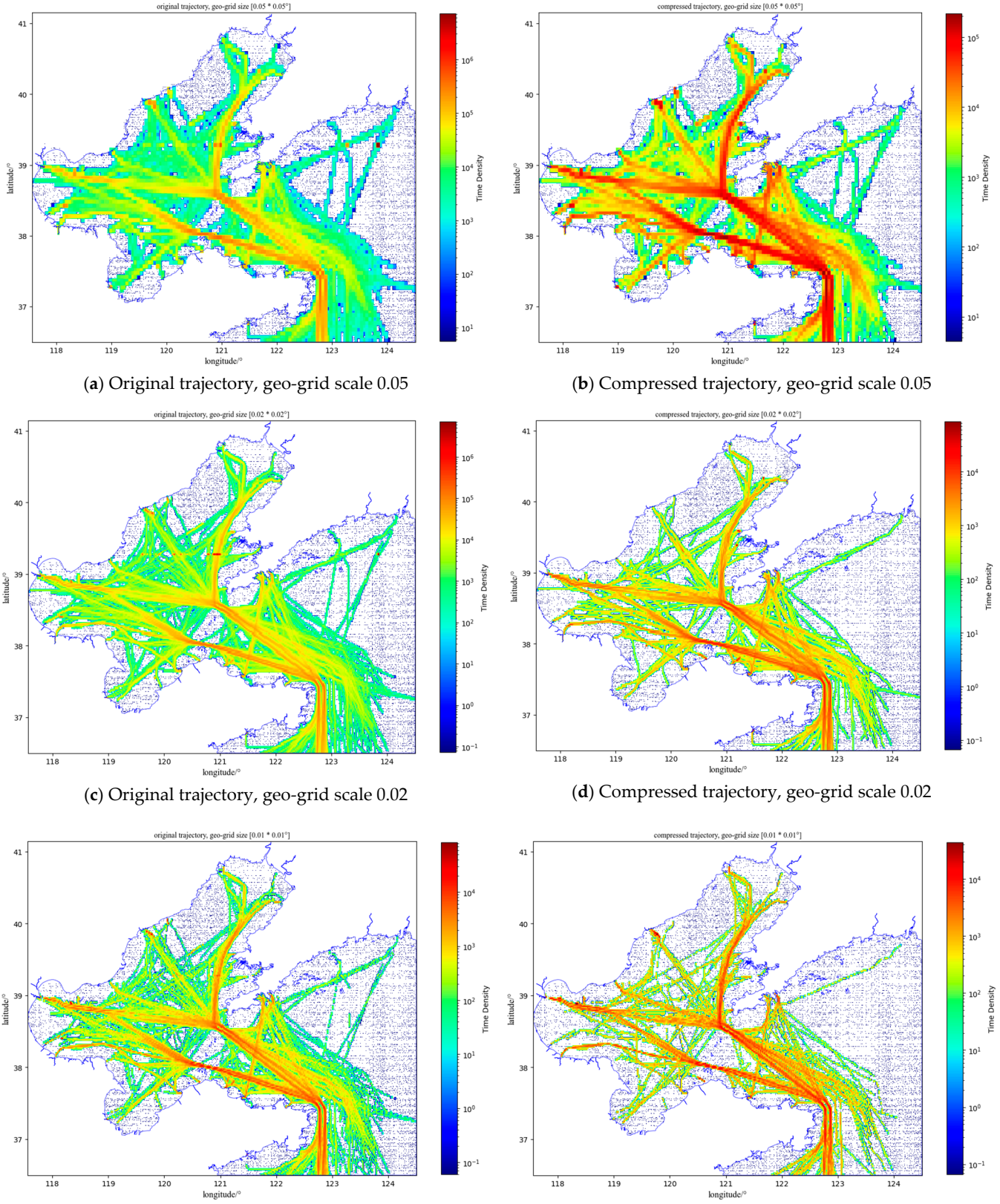

(**a**) Original trajectory, geo-grid scale 0.05

(**b**) Compressed trajectory, geo-grid scale 0.05

(**c**) Original trajectory, geo-grid scale 0.02

(**d**) Compressed trajectory, geo-grid scale 0.02

(**e**) Original trajectory, geo-grid scale 0.01

(**f**) Compressed trajectory, geo-grid scale 0.01

Figure 14. Comparison of temporal density pattern distribution of dynamic trajectories at different scales of geospatial grids.

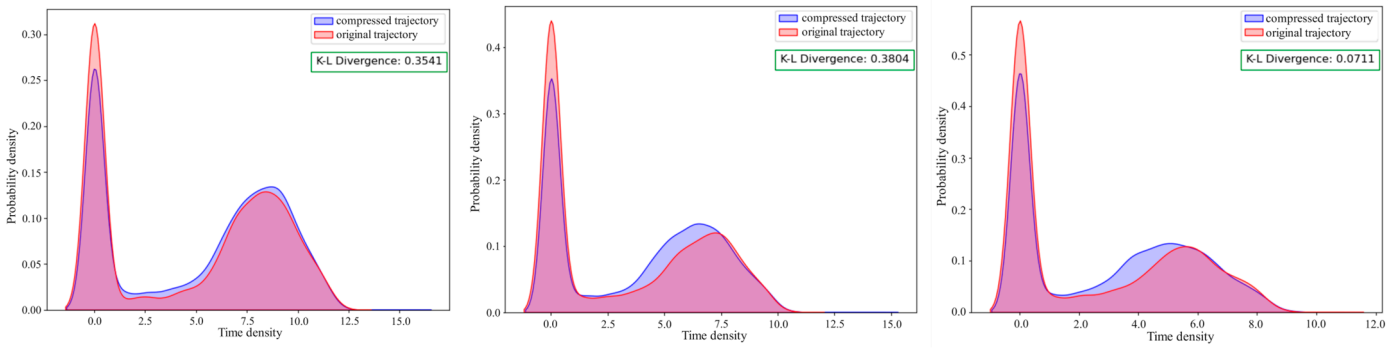

(**a**) Spatial scale is 0.05° (**b**) Spatial scale is 0.02° (**c**) Spatial scale is 0.01°

Figure 15. Probability kernel density distributions of temporal density patterns at different scales corresponding to Figure 14.

5. Conclusions

This study constructs a temporal density model in busy maritime traffic areas. First, the preprocessing operation extracts motion data under the navigation state by removing redundant points such as anchoring and mooring, forming a dynamic trajectory dataset of busy maritime traffic. To ensure each trajectory forms an independent and continuous voyage data sequence, a spatiotemporal segmentation and reconstruction method is proposed, effectively resolving spatiotemporal discontinuities caused by various factors. Second, the designed time window panning trajectory filtering method addresses point jumps and deviations in trajectory data, effectively ensuring temporal continuity while aligning spatial distribution with vessel movement characteristics. This study defines MAOI based on the distribution of busy traffic watersheds with predefined areas, and after vectorizing the MAOI, maps the trajectories onto a gridded representation. Finally, the dynamic trajectory temporal density model integrates the geographical spatial distribution of ship trajectories with their temporal attributes as characteristic criteria, effectively capturing spatiotemporal distribution patterns and identifying spatial density aggregations in maritime traffic. Additionally, the proposed model can effectively identify dynamic trajectory traffic patterns after the application of compression algorithms, offering a new approach to studying the spatiotemporal aggregation of maritime traffic in the era of big data.

6. Discussion and Future Work

In this study, the spatiotemporal segmentation and reconstruction method in Section 3.1 is essential for reducing the impact of redundant data on dynamic trajectory temporal density calculations. The time window panning trajectory filtering method in Section 3.2 effectively mitigates errors such as trajectory jumps and deviations, preserving the spatiotemporal coherence of vessel movements. However, it does not fully address the limitations arising from inaccuracies in raw data positioning. By mapping the temporal characteristics of movement trajectories onto geographic space, this study enhances spatiotemporal association compared to traditional density measurement approaches. However, it does not establish a standardized comparative metric. Future research will focus on time-phase division, spatial scale optimization, and the establishment of metric-based variations to analyze maritime traffic density in marine areas of interest.

Author Contributions: Conceptualization, D.J. and G.S.; Formal analysis, D.J., G.S. and X.W.; Investigation, D.J., G.Z. and W.L.; Methodology, D.J. and L.M.; Supervision, X.W. and G.Z.; Visualization, D.J. and L.M.; Writing—original draft, D.J. All authors have read and agreed to the published version of the manuscript.

Funding: This research was supported by National Science Foundation of China (52101399) and the Fundamental Research Funds for the Central Universities (3132023153).

Institutional Review Board Statement: Not applicable.

Informed Consent Statement: Not applicable.

Data Availability Statement: The original contributions presented in this study are included in the article. Further inquiries can be directed to the corresponding author.

Acknowledgments: We are especially grateful for the financial and data support provided by the Navigation Safety and Guarantee Institute.

Conflicts of Interest: The authors declare no conflicts of interest.

References

1. Chen, X.; Zheng, J.; Li, C.; Wu, B.; Wu, H.; Montewka, J. Maritime traffic situation awareness analysis via high-fidelity ship imaging trajectory. *Multimed. Tools Appl.* **2024**, *83*, 48907–48923. [CrossRef]
2. Lee, J.S.; Kim, T.H.; Park, Y.G. Maritime Transport Network in Korea: Spatial-Temporal Density and Path Planning. *J. Mar. Sci. Eng.* **2023**, *11*, 2364. [CrossRef]
3. Wang, H.B. Safety Risk Assessment Model and Simulation for High-density Ship Traffic. *J. Coast. Res.* **2019**, *93*, 905–910. [CrossRef]
4. Feng, Z.; Yang, H.; Li, X.; Li, Y.; Liu, Z.; Liu, R.W. Real-Time Vessel Trajectory Data-Based Collison Risk Assessment in Crowded Inland Waterways. In Proceedings of the 2019 IEEE 4th International Conference on Big Data Analytics (ICBDA), Suzhou, China, 15–18 March 2019; pp. 128–134. [CrossRef]
5. Zhen, R.; Shi, Z.Q.; Shao, Z.P.; Liu, J.L. A novel regional collision risk assessment method considering aggregation density under multi-ship encounter situations. *J. Navig.* **2022**, *75*, 76–94. [CrossRef]
6. Wang, C.; Zhang, X.; Gao, H.; Bashir, M.; Li, H.; Yang, Z. Optimizing anti-collision strategy for MASS: A safe reinforcement learning approach to improve maritime traffic safety. *Ocean Coast. Manag.* **2024**, *253*, 107161. [CrossRef]
7. Krause, K.; Wittrock, F.; Richter, A.; Busch, D.; Bergen, A.; Burrows, J.P.; Freitag, S.; Halbherr, O. Determination of NOx emission rates of inland ships from onshore measurements. *Atmos. Meas. Tech.* **2023**, *16*, 1767–1787. [CrossRef]
8. Peng, X.; Wen, Y.Q.; Wu, L.C.; Xiao, C.S.; Zhou, C.H.; Han, D. A sampling method for calculating regional ship emission inventories. *Transp. Res. Part D-Transp. Environ.* **2020**, *89*, 102617. [CrossRef]
9. Toz, A.C.; Buber, M.; Koseoglu, B.; Sakar, C. An estimation of shipping emissions to analysing air pollution density in the Izmir Bay. *Air Qual. Atmos. Health* **2021**, *14*, 69–81. [CrossRef]
10. Chen, X.; Wu, H.; Han, B.; Liu, W.; Montewka, J.; Liu, R.W. Orientation-aware ship detection via a rotation feature decoupling supported deep learning approach. *Eng. Appl. Artif. Intell.* **2023**, *125*, 106686. [CrossRef]
11. International Maritime Organization. *International Convention for the Safety of Life at Sea (SOLAS)*; 1974, as amended, Chapter V, Regulation 19; IMO: London, UK, 2002.
12. Li, W.; Zhang, H.; Shi, G.; Wang, X.; Desrosiers, R.; Fang, S. A novel algorithm for ship characteristic points extraction based on density clustering. *J. Mar. Eng. Technol.* **2024**, *23*, 281–290. [CrossRef]
13. Huang, I.L.; Lee, M.-C.; Chang, L.; Huang, J.-C. Development and Application of an Advanced Automatic Identification System (AIS)-Based Ship Trajectory Extraction Framework for Maritime Traffic Analysis. *J. Mar. Sci. Eng.* **2024**, *12*, 1672. [CrossRef]
14. Li, H.; Liu, J.; Wu, K.; Yang, Z.; Liu, R.W.; Xiong, N. Spatio-Temporal Vessel Trajectory Clustering Based on Data Mapping and Density. *IEEE Access* **2018**, *6*, 58939–58954. [CrossRef]
15. Rong, H.; Teixeira, A.P.; Guedes Soares, C. Data mining approach to shipping route characterization and anomaly detection based on AIS data. *Ocean Eng.* **2020**, *198*, 106936. [CrossRef]
16. Luo, D.; Chen, P.; Yang, J.; Li, X.; Zhao, Y. A New Classification Method for Ship Trajectories Based on AIS Data. *J. Mar. Sci. Eng.* **2023**, *11*, 1646. [CrossRef]
17. Willems, N.; Scheepens, R.; van de Wetering, H.; van Wijk, J.J. Visualization of Vessel Traffic. In *Situation Awareness with Systems of Systems*; Springer: New York, NY, USA, 2013; pp. 1–10. [CrossRef]
18. Meng, Q.; Weng, J.; Li, S. Analysis with Automatic Identification System Data of Vessel Traffic Characteristics in the Singapore Strait. *Transp. Res. Record.* **2014**, *2426*, 33–43. [CrossRef]
19. Natale, F.; Gibin, M.; Alessandrini, A.; Vespe, M.; Paulrud, A. Mapping Fishing Effort through AIS Data. *PLoS ONE* **2015**, *10*, e0130746. [CrossRef] [PubMed]
20. Li, Y.; Liu, R.W.; Liu, J.; Huang, Y.; Hu, B.; Wang, K. Trajectory compression-guided visualization of spatio-temporal AIS vessel density. In Proceedings of the 2016 8th International Conference on Wireless Communications & Signal Processing (WCSP), Yangzhou, China, 13–15 October 2016; pp. 1–5. [CrossRef]

21. Liu, Z.; Wu, Z.; Zheng, Z. Modelling ship density using a molecular dynamics approach. *J. Navig.* **2020**, *73*, 628–645. [CrossRef]
22. Yang, J.; Ma, L.; Liu, J. Modeling and application of ship density based on ship scale conversion and grid. *Ocean Eng.* **2021**, *237*, 109557. [CrossRef]
23. Lee, J.S.; Lee, H.T.; Cho, I.S. Maritime Traffic Route Detection Framework Based on Statistical Density Analysis From AIS Data Using a Clustering Algorithm. *IEEE Access* **2022**, *10*, 23355–23366. [CrossRef]
24. Lee, J.-S.; Yu, Y.-U. Calculation of categorical route width according to maritime traffic flow data in the Republic of Korea. *J. Mar. Eng. Technol.* **2023**, *22*, 222–232. [CrossRef]
25. Zhao, L.; Shi, G.; Yang, J. Ship Trajectories Pre-processing Based on AIS Data. *J. Navig.* **2018**, *71*, 1210–1230. [CrossRef]
26. Huang, L.; Zhang, Z.-H.; Wen, Y.-Q.; Zhu, M.; Huang, Y.-M. Stopping behavior recognition and classification of ship based on trajectory characteristics. *J. Traffic Transp. Eng.* **2021**, *21*, 189–198. [CrossRef]
27. Li, Q.; Zheng, Y.; Xie, X.; Chen, Y.; Liu, W.; Ma, W.-Y. Mining user similarity based on location history. In Proceedings of the 16th ACM SIGSPATIAL International Conference on Advances in Geographic Information Systems, New York, NY, USA, 5–7 November 2008; p. 10. [CrossRef]
28. Tran, L.H.; Quoc, N.; Hung, V.; Do, N.H.; Yan, Z. Robust and Hierarchical Stop Discovery in Sparse and Diverse Trajectories. *EPFL*. 2011, pp. 1–10. Available online: https://infoscience.epfl.ch/record/175473 (accessed on 10 July 2024).
29. Zhao, W.; Hu, Z.; Wei, C. Ship sailing period identification based on ais. *Comput. Appl. Softw.* **2018**, *35*, 111–116.
30. Tam, J.H. Overview of performing shore-to-ship and ship-to-ship compatibility studies for LNG bunker vessels. *J. Mar. Eng. Technol.* **2022**, *21*, 257–270. [CrossRef]
31. Guan, M.; Cao, Y.; Cheng, X. Research of AIS Data-Driven Ship Arrival Time at Anchorage Prediction. *IEEE Sensors J.* **2024**, *24*, 12740–12746. [CrossRef]
32. Jiang, D.; Shi, G.; Li, N.; Ma, L.; Li, W.; Shi, J. TRFM-LS: Transformer-Based Deep Learning Method for Vessel Trajectory Prediction. *J. Mar. Sci. Eng.* **2023**, *11*, 880. [CrossRef]
33. Wu, Z.; Zhu, J. *Marine Traffic Engineering*, 2nd ed.; Dalian Maritime University Press: Dalian, China, 2004.
34. Ning, J.; Huang, T.; Diao, B.; Zhao, R.; Bi, J. A fine grained grid-based maritime traffic density algorithm for mass ship trajectory data. *Comput. Eng. Sci.* **2015**, *37*, 2242–2249.
35. Dai, Z.; Zhang, L.; Jia, S.; Pang, H. Shipping Density Assessment Based on Trajectory Big Data. *IOP Conf. Ser. Earth Environ. Sci.* **2019**, *310*, 022032. [CrossRef]
36. The Flanders Marine Institute. Marineregions.org, Maritime Boundaries (Latest Version). 2023. Available online: https://marineregions.org/sources.php (accessed on 15 October 2024).
37. Douglas, D.H.; Peucker, T.K. Algorithms for the reduction of the number of points required to represent a digitized line or its caricature. *Can. Cartogr.* **1973**, *10*, 112–122. [CrossRef]
38. Wei, Z.; Xie, X.; Zhang, X. AIS trajectory simplification algorithm considering ship behaviours. *Ocean Eng.* **2020**, *216*, 108086. [CrossRef]
39. Gao, C.; Zhao, Y.; Wu, R.; Yang, Q.; Shao, J. Semantic trajectory compression via multi-resolution synchronization-based clustering. *Knowl. Based Syst.* **2019**, *174*, 177–193. [CrossRef]
40. Gao, M.; Shi, G.-Y.; Li, W.-F. Online compression algorithm of AIS trajectory data based on improved sliding window. *J. Traffic Transp. Eng.* **2018**, *18*, 218–227. [CrossRef]
41. Ma, L.; Shi, G.; Li, W.; Jiang, D. A Direction-Preserved Vessel Trajectory Compression Algorithm Based on Open Window. *J. Mar. Sci. Eng.* **2023**, *11*, 2362. [CrossRef]
42. Tang, C.H.; Wang, H.; Zhao, J.H.; Tang, Y.Q.; Yan, H.R.; Xiao, Y.J. A method for compressing AIS trajectory data based on the adaptive-threshold Douglas-Peucker algorithm. *Ocean Eng.* **2021**, *232*, 109041. [CrossRef]